



# HHS Public Access

Author manuscript

*Mol Genet Metab.* Author manuscript; available in PMC 2016 December 01.

Published in final edited form as:

*Mol Genet Metab.* 2015 December ; 116(4): 289–297. doi:10.1016/j.ymgme.2015.10.012.

## Pallidal neuronal apolipoprotein E in pantothenate kinase-associated neurodegeneration recapitulates ischemic injury to the globuspallidus

Randall L. Woltjer, MD, PhD<sup>1</sup>, Lindsay C. Reese, PhD<sup>1</sup>, Brian E. Richardson, PhD<sup>2</sup>, Huong Tran, BS<sup>1</sup>, Sarah Green, BS<sup>1</sup>, Thao Pham<sup>1</sup>, Megan Chalupsky<sup>1</sup>, Isabella Gabriel<sup>1</sup>, Tyler Light<sup>1</sup>, Lynn Sanford, BS<sup>2</sup>, Suh Y. Jeong, PhD<sup>2</sup>, Jeffrey Hamada, BS<sup>2</sup>, Leila K. Schwanemann<sup>2</sup>, Caleb Rogers, MD<sup>2</sup>, Allison Gregory, MS, CGC<sup>2</sup>, Penelope Hogarth, MD<sup>2</sup>, and Susan J. Hayflick, MD<sup>2</sup>

<sup>1</sup>Department of Pathology, Oregon Health & Science University, Portland, Oregon 97239

<sup>2</sup>Department of Molecular and Medical Genetics, Oregon Health & Science University, Portland, Oregon 97239

### Abstract

Pantothenate kinase-associated neurodegeneration (PKAN) is a progressive movement disorder that is due to mutations in *PANK2*. Pathologically, it is a member of a class of diseases known as neurodegeneration with brain iron accumulation (NBIA) and features increased tissue iron and ubiquitinated proteinaceous aggregates in the globuspallidus. We have previously determined that these aggregates represent condensed residue derived from degenerated pallidal neurons.

However, the protein content, other than ubiquitin, of these aggregates remains unknown. In the present study, we performed biochemical and immunohistochemical studies to characterize these aggregates and found them to be enriched in apolipoprotein E that is poorly soluble in detergent solutions. However, we did not determine a significant association between *APOE* genotype and the clinical phenotype of disease in our database of 81 cases. Rather, we frequently identified similar ubiquitin- and apolipoprotein E-enriched lesions in these neurons in non-PKAN patients in the penumbrae of remote infarcts that involve the globuspallidus, and occasionally in other brain sites that contain large  $\gamma$ -aminobutyric acid (GABA)ergic neurons. Our findings, taken together, suggest that tissue or cellular hypoxic/ischemic injury within the globuspallidus may underlie the pathogenesis of PKAN.

### Keywords

Pantothenate kinase-associated neurodegeneration; apolipoprotein E; globuspallidus

---

Corresponding author: Randall Woltjer, MD, PhD, Department of Pathology, Mail code L113, 3181 SW Sam Jackson Park Road, Oregon Health & Science University, Portland, Oregon 97239. woltjerr@ohsu.edu.

**Publisher's Disclaimer:** This is a PDF file of an unedited manuscript that has been accepted for publication. As a service to our customers we are providing this early version of the manuscript. The manuscript will undergo copyediting, typesetting, and review of the resulting proof before it is published in its final citable form. Please note that during the production process errors may be discovered which could affect the content, and all legal disclaimers that apply to the journal pertain.

## 1. Introduction

Pantothenate kinase-associated neurodegeneration (PKAN) is the most common subtype of a spectrum of diseases known collectively as neurodegeneration with brain iron accumulation (NBIA) (Gregory and Hayflick, 2013). Common clinical symptoms in PKAN include parkinsonism with generalized dystonias that typically begin in childhood with a progressively disabling and ultimately fatal course (Gregory and Hayflick, 2002). Cognitive function in PKAN is relatively intact (Freeman *et al.*, 2007). Diagnosis is enabled by magnetic resonance imaging (MRI), which reveals a characteristic “eye of the tiger” appearance with a T2 hyperintense signal core surrounded by a hypointense region in the globus pallidus, which is compatible with the clinical phenotype of a predominantly movement disorder (Hayflick *et al.*, 2003).

Histologically, all NBIA disorders feature iron accumulation in the basal ganglia with neuroaxonal spheroids (Kruer, 2013). Additional neuropathologic features may be specific to NBIA subtypes and include Lewy bodies and neurofibrillary tangles (Kruer, 2013). As the genetic bases of NBIA disorders have been elucidated, the specificity of these features has become more apparent. PKAN is caused by recessively inherited mutations in *PANK2*, encoding pantothenate kinase 2, a mitochondrial enzyme that functions as the rate-limiting step in coenzyme A (CoA) biosynthesis (Dansie *et al.*, 2014; Hayflick, 2014). *PANK2* serves as a putative sensor of matrix CoA levels for fatty acid  $\beta$ -oxidation (Leonardi *et al.*, 2007). In PKAN, the loss of *PANK2* function would mimic the basal state signaling sufficient CoA independent of matrix CoA status. The functional basis of the association of this defect with clinical and pathologic disease, in particular the localization to the basal ganglia, remains unknown (Hayflick, 2014).

We recently reported detailed histologic features in the brain autopsies of six patients with genetically confirmed PKAN (Kruer *et al.*, 2011). Specifically, we observed iron deposition and neuroaxonal spheroids in the globus pallidus, as described above, but no specific or significant features of other neurodegenerative diseases, such as amyloid plaques, neurofibrillary tangles, or Lewy bodies. Antibodies to ubiquitin strongly labeled proteinaceous aggregates found in structures that we identified as degenerating globus pallidus neurons. However, in keeping with the absence in PKAN of other histopathologic lesions found in other neurodegenerative diseases, convincingly positive staining for tau,  $\alpha$ -synuclein,  $\beta$ -amyloid, or TAR DNA-binding protein 43 (TDP-43) failed to co-localize with ubiquitin expression in degenerating neurons.

We report here that ubiquitin expression in inclusions of degenerating pallidal neurons in PKAN brain tissue co-localizes with apolipoprotein E (apoE). The detergent-insoluble fraction of tissue extracts from PKAN patients was found to be enriched in apoE; insolubility in detergent solutions is a biochemical feature common to abnormal misfolded protein species found in other neurodegenerative diseases (Woltjer *et al.*, 2009). No *APOE* allele-specific association with PKAN phenotype severity was evident. Morphologically identical inclusions were identified in degenerating neurons in the vicinity of remote infarcts in the globus pallidus in non-PKAN patients, and these were also found to contain ubiquitin

and apoE. These findings indicate that the pathologic phenotype of PKAN recapitulates that of chronic neuronal hypoxia and/or ischemia involving the globus pallidus.

## 2. Materials and methods

### 2.1. Human subjects

Subjects were enrolled pre- or post-mortem after consent was obtained from surviving family members. The brain autopsies of most subjects were performed at Oregon Health & Science University (OHSU) in accordance with the requirements of the local Institutional Review Board, with informed consent for brain autopsy obtained from the legal next of kin. Other tissue samples were obtained from the National Institute of Child Health and Human Development Brain and Tissue Bank for Developmental Disorders, administered at the University of Maryland. Patient histories were obtained via direct interview, review of medical records, and/or correspondence with surviving family members.

### 2.2. APOE genotyping

Patient *APOE* genotypes were determined by polymerase chain reaction (PCR) amplification of genomic DNA and sequencing. Primers were designed to amplify exon 4 of *APOE*, and sequences were determined by the OCTRI Sequencing Core at OHSU using a 3130XL Genetic Analyzer (Applied Biosystems, Foster City, CA).

Patients were classified as classic or atypical PKAN using published criteria (Hayflick, 2013). The frequencies of *APOE* E2, E3, and E4 alleles in patients with classic or atypical PKAN were compared to each other as well as to published frequencies in the general population and analyzed by chi-square tests. General population frequencies were obtained from a meta-analysis compiled by AlzGene (Bertram *et al.*, 2007).

### 2.3. Postmortem tissue processing

Fixed tissue was prepared by immersion of brain tissue from PKAN and non-PKAN patients in 10% neutral buffered formalin for at least ten days, followed by dissection into sections containing the basal ganglia and other brain regions.

### 2.4. Histologic and immunohistochemical evaluation

Standard methods were used to prepare 6- $\mu$ m paraffin-embedded sections, that were stained with hematoxylin and eosin (H&E) with luxol fast blue (LFB) myelin stain to evaluate the presence of characteristic PKAN-associated findings.

Immunohistochemical stains were applied to paraffin sections after deparaffinization and antigen retrieval (5 min treatment at room temperature with 95% formic acid, followed by 30 min incubation in citrate buffer [pH 6.0] at 90°C). Tissue sections were blocked with 5% nonfat dry milk in phosphate-buffered saline and labeled with antibodies to ubiquitin (Dako, Glostrup, Denmark) and apoE (Academy Biomedical, Houston, TX) (Holthofer *et al.*, 1982). All antibodies were applied at 1:5,000 dilution. Results were visualized after application of appropriate secondary antibodies using diaminobenzidine (brown) or Vector Red (Vector Laboratories) as chromagens.

## 2.5. Immunofluorescent imaging

The 6- $\mu\text{m}$  tissue sections were deparaffinized and subjected to antigen retrieval as described above. Tissue sections were blocked with 10% bovine serum albumin (BSA) and simultaneously incubated with antibodies against ubiquitin (1:5,000, Invitrogen/Life Technologies, Carlsbad, CA) and apoE (1:10,000, Biomedical, Houston, TX) diluted in 1% BSA. Antibody labeling was visualized using Alexa-conjugated fluorescent secondary antibodies (1:500, Life Technologies). Sections were mounted using Prolong Gold antifade agent with 4',6-diamidino-2-phenylindole (DAPI, Life Technologies). Tissue was imaged using a Zeiss LSM 780 confocal microscope (Carl Zeiss, Oberkochen, Germany) at the OHSU Advanced Light Microscopy core facility.

## 2.6. Biochemical characterization of apoE

For biochemical studies performed on fresh frozen tissue, archived frozen globuspallidus from PKAN and non-PKAN control subjects was thawed, and proteins were liberated by probe sonication in 10 mL denaturing tissue lysis buffer containing 62.5 mM Tris (pH 6.8), 2% sodium dodecyl sulfate (SDS), and 10% glycerol per gram tissue. Extracts were separated by centrifugation for 10 min at  $14,000 \times g$ , and protein assays of supernatants were performed in triplicate using standard methods (Pierce BCA Protein Assay Kit, Thermo Fisher Scientific Inc., Rockford, IL). Tissue protein was normalized to 2 mg/mL, Dithiothreitol (DTT) was added to a final concentration of 50 mM, and bromophenol blue was added to 0.01%. This method afforded near complete tissue protein extraction in extracts of known protein concentration in commonly used denaturing gel electrophoresis sample buffer (Laemmli, 1970). Sodium dodecyl sulfate (SDS)-polyacrylamide gel electrophoresis, transfer to polyvinylidenedifluoride (PVDF) membranes, and immunoblotting for apoE were performed on 40  $\mu\text{g}$  total extracted protein using standard methods (Laemmli, 1970).

To prepare detergent-insoluble extracts of tissue, ten volume sice-cold 100 mM Tris, (pH 7.4)/10% sucrose “buffer A” containing protease and phosphatase inhibitors was added per gram tissue samples as previously described (Yang *et al.*, 2007) The tissue was sonicated with a probe sonicator for 30 s and then separated by ultracentrifugation at  $450,000 \times g$  for 20 min at 4°C. Supernatants were removed, and three subsequent serial extractions of the insoluble pellets were performed with the same volume of buffer A with 1% Triton X-100 followed by ultracentrifugation at each step. The remaining pellets were resuspended in 10 mM Tris, (pH 8.0) to remove residual detergent, and the detergent-insoluble proteins were liberated from the final pellet by sonication in 70% formic acid. Aliquots of extracted protein were dried by vacuum centrifugation and resolubilized by sonication in 5 M guanidine hydrochloride and 100 mM Tris (pH 8.0) in a volume equal to the original extract volume. Enzyme-linked immunosorbent assays (ELISAs) to quantify apoE and ubiquitin were performed using 200 ng total detergent-insoluble protein per assay as previously described (Woltjer *et al.*, 2009)

ApoE was immunoprecipitated from the detergent-insoluble protein fraction after resolubilization in guanidine as described above. The 40- $\mu\text{L}$  resolubilized samples were first diluted with 10 volumes Tris-buffered saline (pH 7.4) containing 0.1% Tween 20 detergent

(TBST), followed by the addition of 10  $\mu$ L anti-apoE antibody and 40  $\mu$ L agarose-bound protein G slurry (Santa Cruz Biotechnology, Santa Cruz, CA). After incubation with gentle agitation for 1 h at 4°C, agarose beads and associated immunoprecipitated material were collected by centrifugation for 5 min at 500 $\times$  g at 4 degrees C, the supernatants were discarded, and agarose-bound immunoprecipitates were washed by resuspension in 1 m Lysine-cold TBST. After 4 washes, the beads were eluted by the addition of 20 mM ethanolamine (pH 12.5) and centrifugation as described above, and the eluates (supernatants) were collected. These were neutralized with the addition of 256 volumes of 100 mM Tris (pH 8.0). To confirm the specificity of immunoprecipitation, additional triplicate immunoprecipitations of Tris/guanidine buffer without brain extracts were prepared in parallel and washed and eluted exactly as described above for brain extracts. ELISAs for ubiquitin were performed from 200  $\mu$ L neutralized immunoprecipitates as previously describe (Woltjer *et al.*, 2009).

### 2.7. Statistical methods

Statistical analyses were carried out using Prism software (GraphPad Software, Inc., La Jolla, CA) unless otherwise noted.

## 3. Results

### 3.1. Patient characterization

All PKAN subjects had typical clinical, imaging, and histologic features as described previously, including ubiquitin-positive degenerating neurons in the globus pallidus (Kruer *et al.*, 2011). The clinical and molecular features of PKAN subjects whose tissues were used in biochemical and histochemical studies are summarized in Table 1.

Tissue from patients without evidence of neurodegenerative disease or with clinically diagnosed and neuropathologically confirmed Alzheimer's disease was used for protein biochemical studies. For immunohistochemical studies of remote infarcts, we used tissue from elderly patients with grossly ascertained and microscopically confirmed brain lesions without additional neurodegenerative disease. Patients with neurologic disease were clinically evaluated in the OHSU Layton Aging and Alzheimer's Disease Center as previously described (Silbert *et al.*, 2008). Brain tissue from all non-PKAN cases was obtained from the Oregon Brain Bank and selected based on diagnoses of ischemic injury, infarction, and neurodegenerative disease as established by standard histopathologic assessment performed by the Neuropathology Core of the Layton Aging and Alzheimer's Disease Center.

### 3.2. Immunohistochemical characterization

The globus pallidus, specifically the interna, was most heavily affected in PKAN brain, as previously described (Kruer *et al.*, 2011). H&E-stained sections showed rarefied brain parenchyma with iron deposits, gliosis, and variably compact eosinophilic spheroidal structures that roughly approximated the size and spacing of large pallidal neurons (Fig. 1A) (Kruer *et al.*, 2011). We immunohistochemically confirmed the presence of ubiquitin in these structures (Fig. 1B) in all cases. The presence of apoE was also established by

immunohistochemical labeling and was found in degenerating neurons in a distribution that was similar to that of ubiquitin (Fig. 1C). In addition, apoE expression was increased in reactive astrocytes, the major apoE-expressing cells of the brain (Boyles *et al.*, 1985; Pitas *et al.*, 1987; Grehan *et al.*, 2001). No abnormal apoE expression was identified in globus pallidus tissue from age-matched control subjects who died without neurologic disease.

ApoE- and ubiquitin-positive structures were widespread throughout the globus pallidus in PKAN but displayed a variety of morphologies. Granular clusters were found only in the globus pallidus interna and likely represent remnants of more disintegrated neurons in the area of maximal tissue damage that corresponds to the “eye of the tiger” sign seen in MRI scans. Compact or aggregated structures were more widespread throughout the globus pallidus along a morphologic spectrum that suggests progressive aggregation and ubiquitination of apoE in intermediate to advanced stages of neuronal degeneration.

### 3.3. Immunofluorescent labeling of neuronal aggregated protein in PKAN

Next, dual-label confocal immunofluorescence was performed on paraffin sections of PKAN globus pallidus. The results confirmed the presence of apoE in ubiquitin-positive structures (Fig. 2). In addition, occasional less compact inclusions were identified, typically at the periphery of the most heavily affected areas of the globus pallidus. These inclusions were compatible with less developed lesions and were variably positive for ubiquitin but strongly positive for apoE. Occasionally, DAPI-positive nuclear material was associated with these aggregates, confirming their localization to cell bodies rather than neuronal processes, as we previously ascertained (Kruer *et al.*, 2011). The findings are compatible with the interpretation that apoE aberrantly accumulates in PKAN neurons and that a large subset of aggregated apoE is ubiquitinated or associated with another ubiquitinated protein to constitute the hallmark cellular lesion of PKAN.

### 3.4. Biochemical characterization of apoE protein in PKAN

Aggregated proteins in morphologically identifiable lesions are common in many neurodegenerative diseases including Alzheimer’s disease, Parkinson’s disease, and various forms of frontotemporal lobar degeneration; these proteinaceous deposits are attributed to cellular processes that lead to protein damage, inducing misfolding that typically results in reduced solubility of accumulated protein in detergent solutions (Woltjer *et al.*, 2009). To determine whether this is true of apoE in the PKAN globus pallidus, we prepared total (sodium dodecyl sulfate, or SDS-extracted) and detergent (Triton X-100)-insoluble fractions of this brain region from PKAN and control subjects and performed western blotting and ELISAs on these extracts. ApoE was increased in PKAN subjects compared to controls in both SDS extracts of total globus pallidus protein (Fig. 3A and 3B) and detergent-insoluble extracts (Fig. 3C). Despite the presence of occasional apoE-positive beta-amyloid plaques in the deep gray matter in the brains of Alzheimer’s disease patients, detergent-insoluble apoE was not significantly increased in eight patients with Alzheimer’s disease who were included as controls for nonspecific tissue effects of other neurodegenerative disease. There was no increased ubiquitin ELISA signal in PKAN compared to control groups (Fig. 3D); this could be due to lower antibody sensitivity compared to that used for apoE ELISAs, a

smaller tissue amount of abnormal ubiquitin compared to apoE, or a combination of these factors. To increase assay sensitivity and specificity, we immunoprecipitated apoE from detergent-insoluble fractions of PKAN and control globospallidus prior and performed ELISAs to determine the ubiquitin content of immunoprecipitates (Fig. 3E). This method revealed increased ubiquitin signal in samples from PKAN patients compared to controls, which is consistent with ubiquitination of apoE or a co-immunoprecipitating apoE-associated protein species in PKAN compared to controls. It should be noted that the association of any co-immunoprecipitating proteins would be very tight, having been maintained throughout the detergent and formic acid extraction, and guanidine resolubilization, steps.

### 3.5. APOE genotype and PKAN phenotype

The  $\epsilon 4$  allele of *APOE* is associated with an increased risk of various neurodegenerative diseases, most notably Alzheimer's disease. To determine whether the presence of the  $\epsilon 4$  allele was associated with PKAN, we determined *APOE* genotypes in the known available population of patients with classic or atypical PKAN. The classic PKAN group (n=81) had an allele distribution of 9  $\epsilon 2$  (5.6%), 140  $\epsilon 3$  (86.4%), and 13  $\epsilon 4$  (8%). The atypical PKAN group (n=41) had an allele distribution of 6  $\epsilon 2$  (7.3%), 70  $\epsilon 3$  (85.4%), and 6  $\epsilon 4$  (7.3%). Chi-square analysis revealed that none of the allele frequencies differed significantly: atypical versus classic PKAN allele frequencies (p=0.26), atypical PKAN versus general population frequencies (p=0.58), and classic PKAN versus general population frequencies (p=0.06). We also did not detect an association of age of onset or death with *APOE* genotype in these populations (data not shown); nor, in our limited patient set, was there an obvious association between the nature of the genetic lesion (in-frame deletion, missense, or premature stop codon) and the amount of detergent-insoluble apoE.

### 3.6. Recapitulation of ubiquitin- and apoE-positive aggregates in chronic hypoxic/ischemic injury affecting the globospallidus

Neuronal changes that resemble those found in PKAN were serendipitously recognized in globospallidi from elderly patients with vascular ischemic injury. Typically, these were observed in the penumbrae of medium-sized subacute and older infarcts (Fig. 4A). The spectrum of neuronal changes was similar to that observed in PKAN and ranged from neurons with recognizable morphology and dense, eosinophilic cytoplasm to structures that were no longer recognizable as neurons but contained more compact aggregated proteinaceous deposits of similar size and eosinophilic staining (Fig. 4B and 4C).

Immunohistochemical and immunofluorescent labeling of brain tissue from these subjects revealed a spectrum of ubiquitin- and apoE-positive aggregates that was indistinguishable from lesions observed in PKAN (Fig. 4D–4L), with the exception of the widespread distribution in the globospallidus in PKAN versus circumscribed localization to and around infarcts in non-PKAN subjects.

### 3.7. Identification of PKAN-type protein aggregates in other brain regions

We performed a broad survey of brain tissues containing infarcts in various locations. Small to medium-sized infarcts with similar size and chronicity to those described for the

globuspallidus were sought in subjects who had died without significant additional neurodegenerative disease. Neocortical and hippocampal subacute or older infarcts were not associated with identifiable ubiquitin- or apoE-positive granular aggregates in neurons, although apoE was widely expressed in reactive astrocytes (Fig. 5A) and increased with diffuse cytoplasmic distribution in hippocampal pyramidal and other neurons, including those of the globuspallidus, that displayed other morphologic features such as cytoplasmic contraction and hyper eosinophilia associated with acute hypoxic/ischemic injury (Fig. 5B and 5C). However, granular ubiquitin- and apoE-positive protein aggregates similar to those of PKAN were observed in neurons in association with remote infarcts in the pars reticulata of the substantianigra (Fig. 5D–5F) and cerebellar Purkinje cells (Fig. 5G–5I). These neuronal populations, like those of the affected neurons of the globuspallidus, are characterized by a relatively large size that supports longer intracerebral projections, as well as GABAergic neurotransmission (Huang *et al.*, 2007; Uusisaari and Knopfel, 2008; Zhou and Lee, 2011).

#### 4. Discussion

Common neurodegenerative diseases such as Alzheimer's disease, Parkinson's disease, other synucleinopathies, and various forms of frontotemporal lobar degeneration are characterized by the deposition of proteinaceous aggregates of specific proteins in cell type- and location-specific distributions that correspond to symptoms attributable to dysfunction involving the brain regions in which these lesions are found (Soto, 2013; Ross and Poirier, 2004). Protein damage, misfolding, and abnormal association are hypothesized to be the basis of aggregate formation. Previously, we determined that decreased tissue protein solubility, another feature of misfolded aggregated protein, was widespread in Alzheimer's disease and even affected proteins for which an abnormal protein distribution was not discernable (Woltjer *et al.*, 2005). However, although many proteins display mild changes in solubility, the most striking changes causing a redistribution of a large percentage of protein into the insoluble tissue fraction were limited to just a few proteins, including beta-amyloid, tau, and apoE in Alzheimer's disease (Woltjer *et al.*, 2005); alpha-synuclein in diseases that feature Lewy bodies, neurites, and specific glial inclusions; and TDP-43 in neurons affected by the most common form of frontotemporal lobar degeneration. All of these proteinaceous deposits, with the exception of the diffuse plaques containing beta-amyloid and apoE in Alzheimer's disease, are associated with co-localization of ubiquitin in their respective pathologic lesions (Mori *et al.*, 1987; Sampathy *et al.*, 2003; Tofaris *et al.*, 2003; Neumann *et al.*, 2006). We previously reported the absence of significant deposition of any of these proteins, with the exception of apoE, in PKAN (Kruer *et al.*, 2011).

The identification of lesions containing aggregated apoE with substantially increased insolubility in PKAN is reminiscent of its properties in Alzheimer's disease, where it appears heavily co-deposited with beta-amyloid in both diffuse and neuritic plaques and in vessels affected by amyloid angiopathy (Nambra *et al.*, 1991; Strittmatter *et al.*, 1993; Kida *et al.*, 1994). However, although dystrophic tau-positive neurites associated with neuritic plaques are ubiquitinated (Perry *et al.*, 1987), to our knowledge this is the first report of neurodegenerative disease that features the co-deposition of ubiquitin and apoE.



ApoE is the major lipoprotein of the brain, where its endogenous function is to traffic lipids and lipophilic substances (Holtzman *et al.*, 2012; Liu *et al.*, 2013). Its most recognized association with disease is as the major genetic risk factor for development of sporadic Alzheimer's disease, in which the  $\epsilon 2$  and  $\epsilon 4$  alleles convey substantially decreased and increased Alzheimer's disease risk, respectively. Among PKAN patients, we found no evidence for an *APOE* allele-specific correlation with phenotype severity. Patients with PKAN harbor a multitude of mutations in *PANK2*, and it is likely that specific mutations determine disease phenotype much more strongly than alleles of *APOE*.

Besides PKAN, significant neuronal expression of apoE has been described for acutely ischemic hippocampal pyramidal and cortical neurons (Xu *et al.*, 1999; Aoki *et al.*, 2003). The degree of expression in these cells correlates with the apparent degree of ischemic injury, as manifested in the degree of cytoplasmic eosinophilia and contraction, with cornuammonis (CA) 1 neurons being most susceptible to injury and showing the greatest degree of apoE expression. Our survey of various brain regions also demonstrated that apoE expression is not found in the form of inclusions in the hippocampus, even in and around infarcts that are commonly encountered at that site in elderly subjects. It is possible that injured hippocampal pyramidal neurons have either a capacity for recovery or are cleared from the tissue through mechanisms that are not available to large GABAergic neurons of the globus pallidus.

Recapitulation of the morphologic and immunohistochemical features of PKAN neurons in the globus pallidus and other brain regions containing remote infarcts suggests that these features are markers of cell death in association with a marked degree of hypoxic/ischemic injury that appears specific to large GABAergic neurons. Neurodegeneration in PKAN may be attributable to cellular-based or tissue hypoxia; the function of *PANK2* in mitochondrial metabolism would be compatible with a flaw in neuronal oxygen utilization and energy production as a plausible outcome of PKAN (Brunetti *et al.*, 2012; Leoni *et al.*, 2012). It is also conceivable that features of CoA activity in brain, apart those that involve oxidative metabolism, could promote morphologic changes that mimic those of tissue hypoxia as a "final pathway" of various toxic mechanisms that involving the globus pallidus, of which ischemic injury is by far the most commonly recognized.

The current results suggest that the specific localization of brain injury in PKAN to the globus pallidus reflects an intrinsic susceptibility of the large collection of GABAergic neurons at that site to injury, but they do not account for the lack of an apparent effect of either clinical or pathological manifestations of PKAN on larger GABAergic neurons at specific locations elsewhere or on the numerous small GABAergic neurons that are abundantly present throughout the brain. It is tempting to speculate that the combination of relatively poor vascular collateralization of the globus pallidus (Wolfram-Gabel and Maillot, 1994) with an intrinsic susceptibility of large GABAergic neurons accounts for the selective degeneration of these cells in PKAN.

Other toxic or metabolic disorders that selectively damage the globus pallidus may inform our understanding of PKAN pathogenesis. These include carbon monoxide poisoning, manganese toxicity, cyanide poisoning, unconjugated hyperbilirubinemia, pyruvate

dehydrogenase deficiency, methylmalonicacidemia, and succinic semialdehyde deficiency. All of these conditions are associated with mitochondrial dysfunction and oxidative stress but preserved glycolysis (Rodrigues *et al.*, 2002; Alonso *et al.*, 2003; Pearl *et al.*, 2004; Head *et al.*, 2005; Prockop and Chichkov, 2007; Leavesley *et al.*, 2008; Hamel, 2011; Patel *et al.*, 2012; Martinez-Finley *et al.*, 2013). Brain MRI scans of patients with these disorders show evidence of cytotoxic edema in the globus pallidus, which is also observed in PKAN. The high baseline firing rate of the large GABAergic neurons in globus pallidus distinguishes them from similar neurons in other regions. Such tonic activity creates high-energy demands, making these cells vulnerable to subacute energy losses that are tolerated by other neurons (Vitek *et al.*, 1999; Johnston and Hoon, 2000).

Currently, no effective treatment exists for PKAN. Although our findings are based on histologic and biochemical analogies between PKAN and ischemic injury, they invite other studies of experimental models of PKAN to determine whether treatments that promote oxygenation or perfusion of the basal ganglia may be effective treatments that could be translated into human therapies. Alternately, several strategies have been proposed or are in development with the goal of enhancing tissue survival or recovery after stroke (Moskowitz *et al.*, 2010); it is conceivable that these might also have efficacy as neuroprotectants in PKAN.

## Acknowledgements

We acknowledge the patients and families whose thoughtful acts led to the procurement of this tissue for our study. We thank the NICHD Brain and Tissue Bank for Developmental Disorders at the University of Maryland, Baltimore, MD, for providing some of the tissues described here. It should be noted that the role of that institution is to collect and distribute tissue; it cannot endorse studies performed or the interpretation of results. This work was made possible with support from the Oregon Clinical and Translational Research Institute (UL1 RR024140 NCR), a component of the National Institutes of Health (NIH) and NIH Roadmap for Medical Research. We thank Otto Szekely, MD for stimulating and insightful discussions.

### Funding

This work was funded by the NBIA Disorders Association (to S.J.H.), with acquisition of brain tissue supported by NIH P30AG008017 (to R.L.W. of the Oregon Alzheimer's Disease Center, directed by Jeffrey Kaye).

## Abbreviations

<b>ApoE</b>	Apolipoprotein E
<b>BSA</b>	bovine serum albumin
<b>CA</b>	cornuammonis
<b>CoA</b>	coenzyme A
<b>DAPI</b>	4',6-diamidino-2-phenylindole
<b>DTT</b>	dithiothreitol
<b>ELISA</b>	enzyme-linked immunosorbent assay
<b>GABA</b>	Gamma-aminobutyric acid
<b>H&amp;E</b>	hematoxylin and eosin

<b>LFB</b>	luxol fast blue
<b>NBIA</b>	Neurodegeneration with brain iron accumulation
<b>OHSU</b>	Oregon Health & Science University
<b>PANK2</b>	Pantothenate kinase, isoform 2
<b>PKAN</b>	Pantothenate kinase-associated neurodegeneration
<b>PVDF</b>	polyvinylidenedifluoride
<b>SDS</b>	sodium dodecyl sulfate
<b>TBST</b>	Tris-buffered saline (pH 7.4) containing 0.1% Tween 20
<b>TDP-43</b>	TAR DNA-binding protein 43

## References

- Alonso JR, Cardellach F, Lopez S, Casademont J, Miro O. Carbon monoxide specifically inhibits cytochrome c oxidase of human mitochondrial respiratory chain. *Pharmacol Toxicol.* 2003; 93:142–146. [PubMed: 12969439]
- Aoki K, Uchihara T, Sanjo N, Nakamura A, Ikeda K, Tsuchiya K, et al. Increased expression of neuronal apolipoprotein E in human brain with cerebral infarction. *Stroke.* 2003; 34:875–880. [PubMed: 12649507]
- Bertram L, McQueen MB, Mullin K, Blacker D, Tanzi RE. Systematic meta-analyses of Alzheimer disease genetic association studies: the AlzGene database. *Nat Genet.* 2007; 39:17–23. [PubMed: 17192785]
- Boyles JK, Pitas RE, Wilson E, Mahley RW, Taylor JM. Apolipoprotein E associated with astrocytic glia of the central nervous system and with nonmyelinating glia of the peripheral nervous system. *J Clin Invest.* 1985; 76:1501–1513. [PubMed: 3932467]
- Brunetti D, Dusi S, Morbin M, Uggetti A, Moda F, D'Amato I, et al. Pantothenate kinase-associated neurodegeneration: altered mitochondria membrane potential and defective respiration in Pank2 knock-out mouse model. *Hum Mol Genet.* 2012; 21:5294–5305. [PubMed: 22983956]
- Dansie LE, Reeves S, Miller K, Zano SP, Frank M, Pate C, et al. Physiological roles of the pantothenate kinases. *Biochem Soc Trans.* 2014; 42:1033–1036. [PubMed: 25109998]
- Doi H, Koyano S, Miyatake S, Matsumoto N, Kameda T, Tomita A, et al. Siblings with the adult-onset slowly progressive type of pantothenate kinase-associated neurodegeneration and a novel mutation, Ile346Ser, in PANK2: clinical features and (99m)Tc-ECD brain perfusion SPECT findings. *J Neurol Sci.* 2010; 290:172–176. [PubMed: 20006850]
- Freeman K, Gregory A, Turner A, Blasco P, Hogarth P, Hayflick S. Intellectual and adaptive behaviour functioning in pantothenate kinase-associated neurodegeneration. *J Intellect Disabil Res.* 2007; 51:417–426. [PubMed: 17493025]
- Gregory, A.; Hayflick, S. Neurodegeneration with Brain Iron Accumulation Disorders Overview. In: Pagon, RA.; Adam, MP.; Ardinger, HH.; Bird, TD.; Dolan, CR.; Fong, CT., et al., editors. *Gene Reviews*. Seattle: University of Washington; 2013. (Updated 2014).
- Gregory, A.; Hayflick, SJ. Pantothenate Kinase-Associated Neurodegeneration. In: Pagon, RA.; Adam, MP.; Ardinger, HH.; Bird, TD.; Dolan, CR.; Fong, CT., et al., editors. *Gene Reviews*. Seattle: University of Washington; 2002. (Updated 2013).
- Grehan S, Tse E, Taylor JM. Two distal downstream enhancers direct expression of the human apolipoprotein E gene to astrocytes in the brain. *J Neurosci.* 2001; 21:812–822. [PubMed: 11157067]
- Hamel J. A review of acute cyanide poisoning with a treatment update. *Crit Care Nurse.* 2011; 31:72–81. [PubMed: 21285466]

- Hayflick SJ. Pantothenate kinase-associated neurodegeneration (formerly Hallervorden-Spatz syndrome). *J Neurol Sci.* 2003; 207:106–107. [PubMed: 12614941]
- Hayflick SJ. Defective pantothenate metabolism and neurodegeneration. *Biochem Soc Trans.* 2014; 42:1063–1068. [PubMed: 25110003]
- Hayflick SJ, Westaway SK, Levinson B, Zhou B, Johnson MA, Ching KH, et al. Genetic, clinical, and radiographic delineation of Hallervorden-Spatz syndrome. *N Engl J Med.* 2003; 348:33–40. [PubMed: 12510040]
- Head RA, Brown RM, Zolkipli Z, Shahdarpuri R, King MD, Clayton PT, et al. Clinical and genetic spectrum of pyruvate dehydrogenase deficiency: dihydrolipoamide acetyltransferase (E2) deficiency. *Ann Neurol.* 2005; 58:234–241. [PubMed: 16049940]
- Holthofer H, Virtanen I, Kariniemi AL, Hormia M, Linder E, Miettinen A. *Ulex europaeus* I lectin as a marker for vascular endothelium in human tissues. *Lab Invest.* 1982; 47:60–66. [PubMed: 6177923]
- Holtzman DM, Herz J, Bu G. Apolipoprotein E and apolipoprotein E receptors: normal biology and roles in Alzheimer disease. *Cold Spring Harb Perspect Med.* 2012; 2:a006312. [PubMed: 22393530]
- Huang ZJ, Di Cristo G, Ango F. Development of GABA innervation in the cerebral and cerebellar cortices. *Nat Rev Neurosci.* 2007; 8:673–686. [PubMed: 17704810]
- Johnston MV, Hoon AH Jr. Possible mechanisms in infants for selective basal ganglia damage from asphyxia, kernicterus, or mitochondrial encephalopathies. *J Child Neurol.* 2000; 15:588–591. [PubMed: 11019789]
- Kida E, Golabek AA, Wisniewski T, Wisniewski KE. Regional differences in apolipoprotein E immunoreactivity in diffuse plaques in Alzheimer's disease brain. *Neurosci Lett.* 1994; 167:73–76. [PubMed: 8177532]
- Kruer MC. The neuropathology of neurodegeneration with brain iron accumulation. *Int Rev Neurobiol.* 2013; 110:165–194. [PubMed: 24209439]
- Kruer MC, Hiken M, Gregory A, Malandrini A, Clark D, Hogarth P, et al. Novel histopathologic findings in molecularly-confirmed pantothenate kinase-associated neurodegeneration. *Brain.* 2011; 134:947–958. [PubMed: 21459825]
- Laemmli UK. Cleavage of structural proteins during the assembly of the head of bacteriophage T4. *Nature.* 1970; 227:680–685. [PubMed: 5432063]
- Leavesley HB, Li L, Prabhakaran K, Borowitz JL, Isom GE. Interaction of cyanide and nitric oxide with cytochrome c oxidase: implications for acute cyanide toxicity. *Toxicol Sci.* 2008; 101:101–111. [PubMed: 17906319]
- Leonardi R, Rock CO, Jackowski S, Zhang Y-M. Activation of human mitochondrial pantothenate kinase 2 by palmitoylcarnitine. *Proc Natl Acad Sci U S A.* 2007; 104:1494–1499. [PubMed: 17242360]
- Leoni V, Strittmatter L, Zorzi G, Zibordi F, Dusi S, Garavaglia B, et al. Metabolic consequences of mitochondrial coenzyme A deficiency in patients with PANK2 mutations. *Mol Genet Metab.* 2012; 105:463–471. [PubMed: 2221393]
- Liu CC, Kanekiyo T, Xu H, Bu G. Apolipoprotein E and Alzheimer disease: risk, mechanisms and therapy. *Nat Rev Neurol.* 2013; 9:106–118. [PubMed: 23296339]
- Martinez-Finley EJ, Gavin CE, Aschner M, Gunter TE. Manganese neurotoxicity and the role of reactive oxygen species. *Free Radic Biol Med.* 2013; 62:65–75. [PubMed: 23395780]
- Mori H, Kondo J, Ihara Y. Ubiquitin is a component of paired helical filaments in Alzheimer's disease. *Science.* 1987; 235:1641–1644. [PubMed: 3029875]
- Moskowitz MA, Lo EH, Iadecola C. The science of stroke: mechanisms in search of treatments. *Neuron.* 2010; 67:181–198. [PubMed: 20670828]
- Namba Y, Tomonaga M, Kawasaki H, Otomo E, Ikeda K. Apolipoprotein E immunoreactivity in cerebral amyloid deposits and neurofibrillary tangles in Alzheimer's disease and kuru plaque amyloid in Creutzfeldt-Jakob disease. *Brain Res.* 1991; 541:163–166. [PubMed: 2029618]
- Neumann M, Sampathu DM, Kwong LK, Truax AC, Micsenyi MC, Chou TT, et al. Ubiquitinated TDP-43 in frontotemporal lobar degeneration and amyotrophic lateral sclerosis. *Science.* 2006; 314:130–133. [PubMed: 17023659]

- Patel KP, O'Brien TW, Subramony SH, Shuster J, Stacpoole PW. The spectrum of pyruvate dehydrogenase complex deficiency: clinical, biochemical and genetic features in 371 patients. *Mol Genet Metab.* 2012; 106:385–394. [PubMed: 22896851]
- Pearl, PL.; Dorsey, AM.; Barrios, ES.; Gibson, KM. Succinic Semialdehyde Dehydrogenase Deficiency. In: Pagon, RA.; Adam, MP.; Ardinger, HH.; Bird, TD.; Dolan, CR.; Fong, CT., et al., editors. *Gene Reviews*. Seattle: University of Washington; 2004. (Updated 2013).
- Perry G, Friedman R, Shaw G, Chau V. Ubiquitin is detected in neurofibrillary tangles and senile plaque neurites of Alzheimer disease brains. *Proc Natl Acad Sci U S A.* 1987; 84:3033–3036. [PubMed: 3033674]
- Pitas RE, Boyles JK, Lee SH, Foss D, Mahley RW. Astrocytes synthesize apolipoprotein E and metabolize apolipoprotein E-containing lipoproteins. *Biochim Biophys Acta.* 1987; 917:148–161. [PubMed: 3539206]
- Prockop LD, Chichkova RI. Carbon monoxide intoxication: an updated review. *J Neurol Sci.* 2007; 262:122–130. [PubMed: 17720201]
- Rodrigues CM, Sola S, Brites D. Bilirubin induces apoptosis via the mitochondrial pathway in developing rat brain neurons. *Hepatology.* 2002; 35:1186–1195. [PubMed: 11981769]
- Ross CA, Poirier MA. Protein aggregation and neurodegenerative disease. *Nat Med.* 2004; (10 Suppl):S10–S17. [PubMed: 15272267]
- Sampathu DM, Giasson BI, Pawlyk AC, Trojanowski JQ, Lee VM. Ubiquitination of alpha-synuclein is not required for formation of pathological inclusions in alpha-synucleinopathies. *Am J Pathol.* 2003; 163:91–100. [PubMed: 12819014]
- Silbert LC, Nelson C, Howieson DB, Moore MM, Kaye JA. Impact of white matter hyperintensity volume progression on rate of cognitive and motor decline. *Neurology.* 2008; 71:108–113. [PubMed: 18606964]
- Soto C. Unfolding the role of protein misfolding in neurodegenerative diseases. *Nat Rev Neurosci.* 2003; 4:49–60. [PubMed: 12511861]
- Strittmatter WJ, Saunders AM, Schmechel D, Pericak-Vance M, Enghild J, Salvesen GS, et al. Apolipoprotein E: high-avidity binding to beta-amyloid and increased frequency of type 4 allele in late-onset familial Alzheimer disease. *Proc Natl Acad Sci U S A.* 1993; 90:1977–1981. [PubMed: 8446617]
- Tofaris GK, Razaq A, Ghetti B, Lilley KS, Spillantini MG. Ubiquitination of alpha-synuclein in Lewy bodies is a pathological event not associated with impairment of proteasome function. *J Biol Chem.* 2003; 278:44405–44411. [PubMed: 12923179]
- Uusisaari M, Knopfel T. GABAergic synaptic communication in the GABAergic and non-GABAergic cells in the deep cerebellar nuclei. *Neuroscience.* 2008; 156:537–549. [PubMed: 18755250]
- Vitek JL, Chockkan V, Zhang JY, Kaneoke Y, Evatt M, DeLong MR, et al. Neuronal activity in the basal ganglia in patients with generalized dystonia and hemiballismus. *Ann Neurol.* 1999; 46:22–35. [PubMed: 10401777]
- Wolfram-Gabel R, Maillot C. Vascular networks of the nucleus lentiformis. *Surg Radiol Anat.* 1994; 16:373–377. [PubMed: 7725192]
- Woltjer RL, Cimino PJ, Boutte AM, Schantz AM, Montine KS, Larson EB, et al. Proteomic determination of widespread detergent-insolubility including A beta but not tau early in the pathogenesis of Alzheimer's disease. *FASEB J.* 2005; 19:1923–1925. [PubMed: 16129700]
- Woltjer RL, Sonnen JA, Sokal I, Rung LG, Yang W, Kjerulf JD, et al. Quantitation and mapping of cerebral detergent-insoluble proteins in the elderly. *Brain Pathol.* 2009; 19:365–374. [PubMed: 18652590]
- Xu PT, Gilbert JR, Qiu HL, Ervin J, Rothrock-Christian TR, Hulette C, et al. Specific regional transcription of apolipoprotein E in human brain neurons. *Am J Pathol.* 1999; 154:601–611. [PubMed: 10027417]
- Yang W, Woltjer RL, Sokal I, Pan C, Wang Y, Brodey M, et al. Quantitative proteomics identifies surfactant-resistant alpha-synuclein in cerebral cortex of Parkinsonism-dementia complex of Guam but not Alzheimer's disease or progressive supranuclear palsy. *Am J Pathol.* 2007; 171:993–1002. [PubMed: 17675576]

Zhou FM, Lee CR. Intrinsic and integrative properties of substantia nigra pars reticulata neurons. *Neuroscience*. 2011; 198:69–94. [PubMed: 21839148]

Author Manuscript

Author Manuscript

Author Manuscript

Author Manuscript

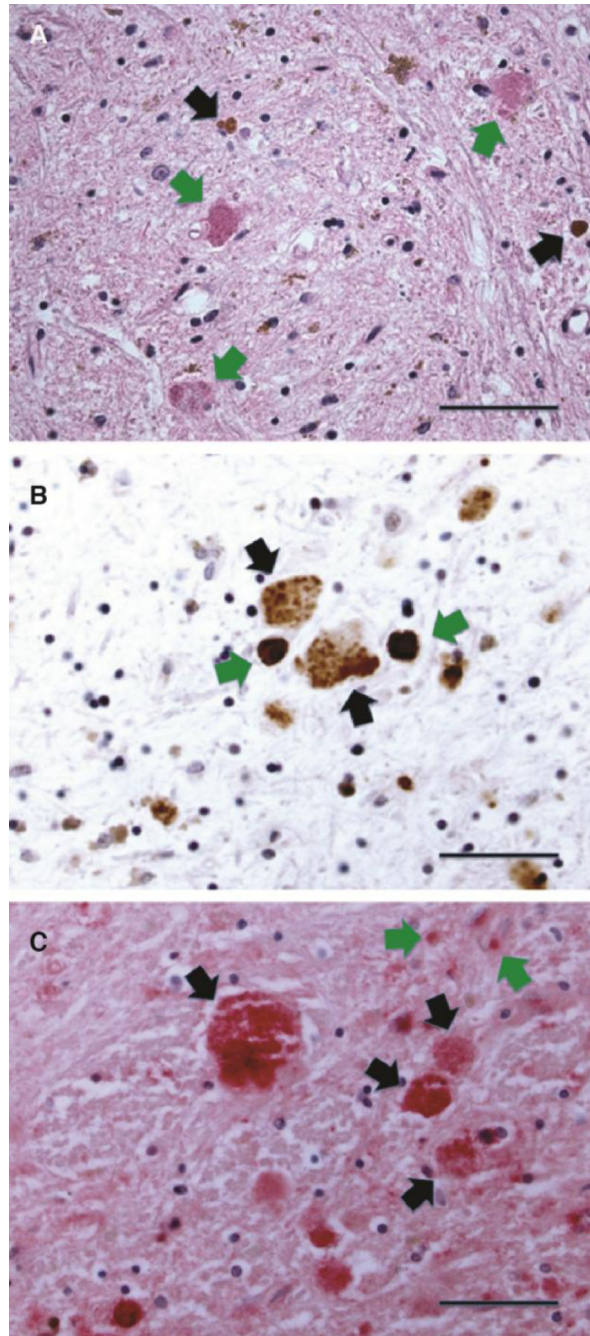


**Figure 1. Histologic and immunohistochemical features of globus pallidus affected by PKAN**  
 (A) High-magnification view of hematoxylin- and eosin (H&E)-stained section of the degenerating neurons harboring eosinophilic proteinaceous aggregates (green arrows). Reactive gliosis and rust-colored iron deposits (black arrows) are present in the background neuropil (scale: 50  $\mu$ m).  
 (B) Ubiquitin-immunohistochemical staining of the globus pallidus in PKAN, highlighting granular ubiquitin-positive inclusions in degenerating neurons (black arrows) as well as more condensed iron deposits (green arrows) (scale: 33  $\mu$ m). Anti-ubiquitin immunostaining

was developed with brown chromagen; hematoxylin counterstain stains background glial nuclei blue.

(C) ApoE-immunohistochemical staining of degenerating neurons in the globus pallidus in PKAN. Staining was developed with Vector Red chromagen to distinguish apoE-positive deposits from brown iron deposits in the background, with hematoxylin as counterstain. Granular proteinaceous material is enriched in apoE (black arrows). Staining in the atrophic neuropil in the background reflects expression by reactive astrocytes (green arrows) (scale: 33  $\mu\text{m}$ ).



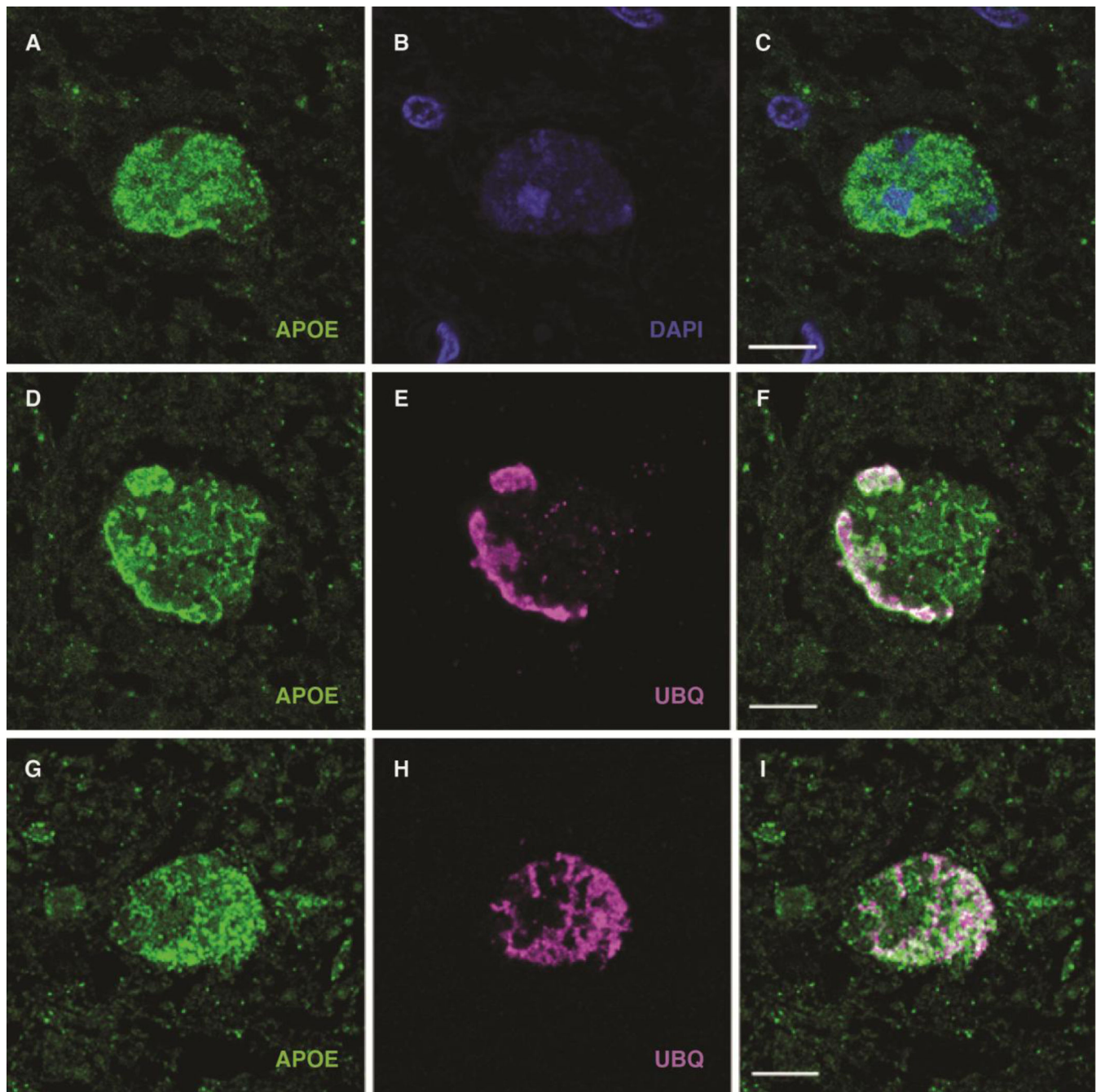


**Figure 2. Demonstration by confocal immunofluorescence of apoE-positive proteinaceous aggregates in the globus pallidus in PKAN**

(A–C) Confocal micrographs of anti-apoE (green) immunofluorescent staining of granular deposits (A), demonstrating widespread cytoplasmic distribution with scant residual DAPI-positive nuclear material (B; A and B merged in C); the size and structure of the apoE-positive material is compatible with cytoplasmic aggregation of apoE in degenerating neurons (scale: 10  $\mu$ m).

(D–I) Association of apoE (green, E and G) and ubiquitin (magenta, E and H, and merged in F and I). D–F demonstrate a degenerating neuron with widespread apoE-containing

aggregates, as well as more densely aggregated apoE on the left aspect of the periphery that feature more intense ubiquitination. G–I depict a neuron with more uniform colocalization of apoE and ubiquitin signals in larger aggregated material throughout the cell (scale: 10  $\mu\text{m}$ ).

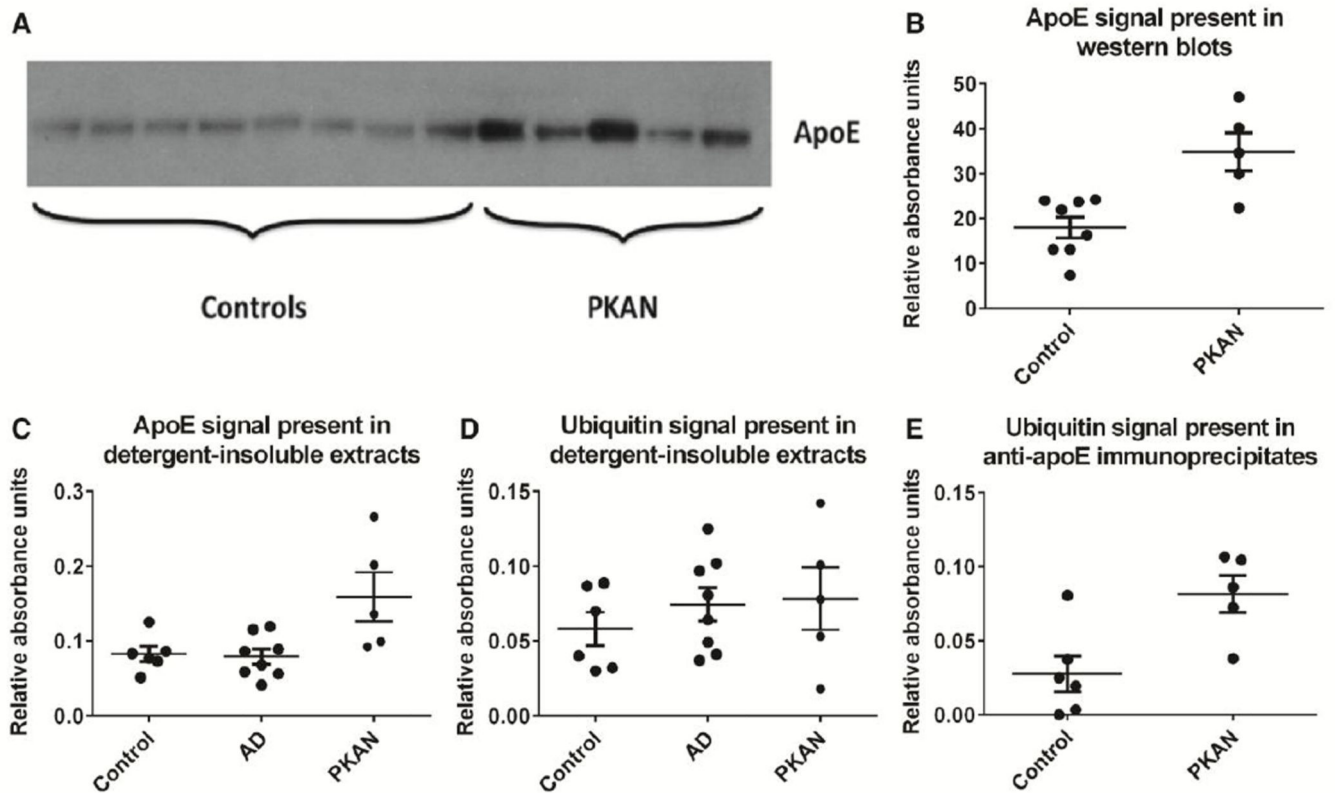


**Figure 3. Biochemical features of apoE in globuspallidus affected by PKAN**

(A) Total SDS-soluble protein was extracted from frozen globuspallidus of eight neurologically intact control and five PKAN patients. Controls ranged in age from 41 to 85 years but these and other experiments did not demonstrate age-related changes in apoE content of the globuspallidus (not shown). ApoE migrated as an approximately 34-kD band in reducing, denaturing SDS gels.

(B) Evaluation of band density using ImageJ software (National Institutes of Health) revealed the total apoE content of the globuspallidus to be significantly increased in PKAN compared to neurologically intact controls (Mann-Whitney test,  $p=0.011$ ). Data are presented as means  $\pm$  SEM.

(C) 200 ng detergent-insoluble protein from six control, eight Alzheimer's disease, and five PKAN patients was subjected to ELISA for quantitative determination of apoE. Control subjects without neurologic disease ranged in age from 41 to 91 years and did not differ significantly in age from AD subjects, who ranged from 56 to 92 years. No association of insoluble apoE was identified as a function of Alzheimer's disease diagnosis (Mann-Whitney test,  $p=0.88$ ) or age of any subject group (not shown). Detergent-insoluble apoE was significantly increased in PKAN subjects compared to controls (Mann-Whitney test,  $p=0.017$ ). Data are presented as means  $\pm$  SEM.

(D) 200 ng detergent-insoluble protein from six control, eight Alzheimer's disease, and five PKAN patients as in C was subjected to ELISA for quantitative determination of ubiquitin. No association of insoluble ubiquitin was identified as a function of patient age or any

diagnosis (Mann-Whitney test,  $p > 0.05$  for all comparisons). Data are presented as means  $\pm$  SEM.

(E) Immunoprecipitation of apoE from detergent-insoluble extracts of globuspallidus from control and PKAN patients was carried out, followed by ELISA determination of the ubiquitin content of immunoprecipitates. Control and PKAN subjects were those of panels C and D. ApoE-associated ubiquitin was significantly increased in extracts from PKAN patients compared to controls (Mann-Whitney test,  $p = 0.017$ ). Data are presented as means  $\pm$  SEM.

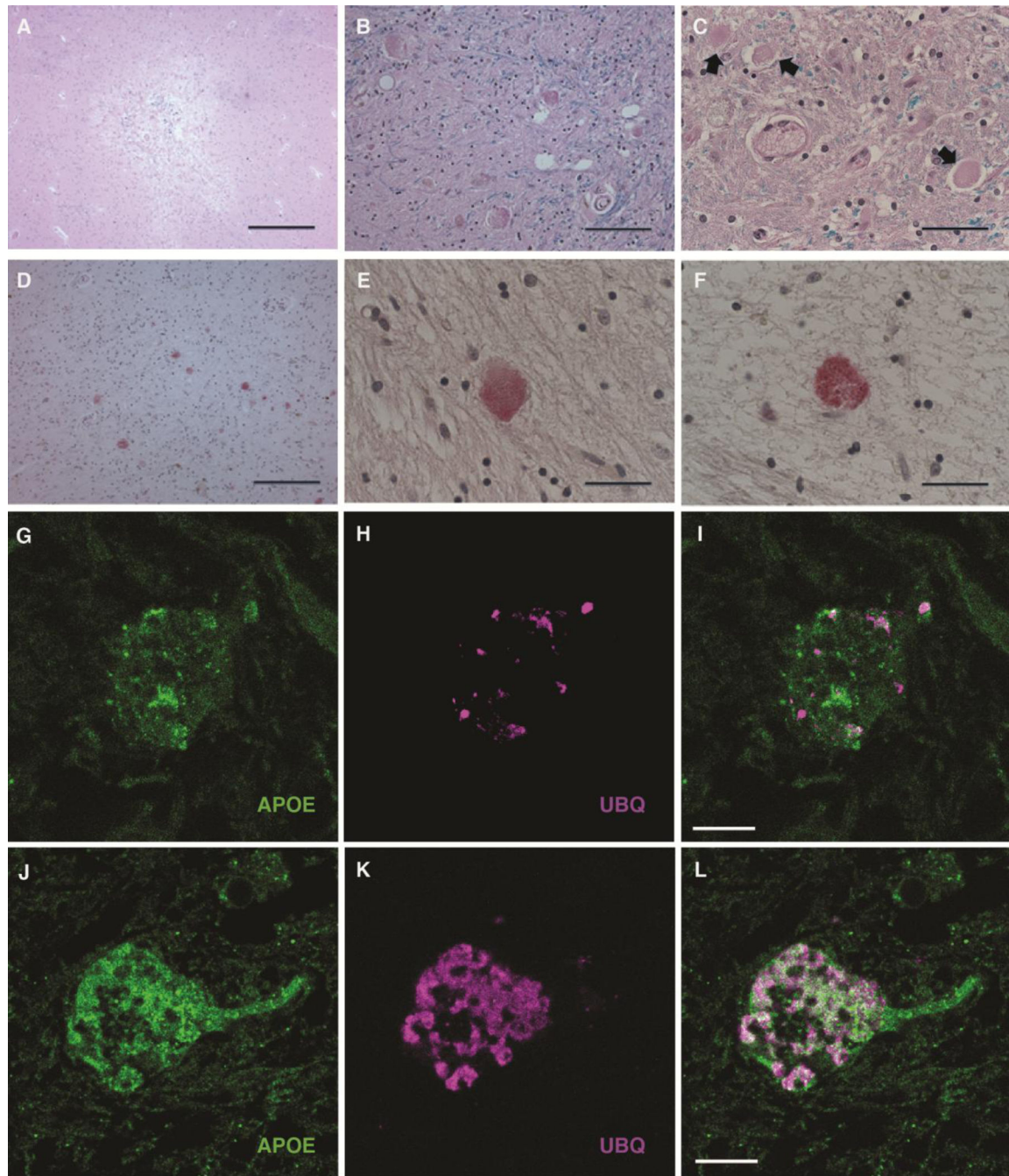


**Figure 4. Association of PKAN-type protein aggregates with chronic hypoxic/ischemic injury involving the globus pallidus**

(A) H&E-stained section of a remote infarct at the interface of the putamen and globus pallidus in an 82-year-old male patient with cognitive impairment attributed to vascular brain injury. Morphologic features that recapitulated findings in PKAN were most commonly encountered at the periphery of lesions of approximately this size and age (scale: 500  $\mu$ m).

(B) Higher magnification of H&E-stained section, with LFB myelin stain, of widespread granular eosinophilic aggregates in the penumbra of a remote ischemic lesion involving the globus pallidus, highly reminiscent of the cellular pathology of PKAN (scale: 50  $\mu\text{m}$ ).

(C) Higher magnification of H&E/LFB stained-section near a subacute ischemic lesion of the globus pallidus in a non-PKAN patient, depicting a spectrum of lesions, ranging from relatively homogeneous eosinophilia in a degenerating neuron (right), to more condensed protein aggregates (center), to eosinophilic granular protein aggregation (left) (scale: 33  $\mu\text{m}$ ).

(D) ApoE immunohistochemical stain of an area of granular degenerating neurons near a remote pallidal infarct in a non-PKAN patient, showing widespread apoE-positive protein aggregates similar to that observed in PKAN (Vector Red development; scale: 100  $\mu\text{m}$ ).

(E) High magnification of anti-apoE immunohistochemical stain of degenerating neuron in the globus pallidus near a remote infarct in a non-PKAN patient (Vector Red development; scale: 33  $\mu\text{m}$ ).

(F) High magnification of anti-ubiquitin immunohistochemical stain of degenerating neuron in the globus pallidus near a remote infarct in a non-PKAN patient, showing increased expression in a pattern very similar to that of apoE (Vector Red development; scale: 33  $\mu\text{m}$ ).

(G–L) Confocal micrographs of degenerating neurons in the globus pallidus of a 56-year old man with a remote infarct, demonstrating association of apoE (green, G and J) and ubiquitin (magenta, H and K, and merged in I and L). G–I depict a neuron with relatively modest apoE expression and focal ubiquitin-positive puncta. J–L demonstrate a degenerating neuron with more widespread apoE- and ubiquitin-containing aggregates, with widespread colocalization (scale: 10  $\mu\text{m}$ ).

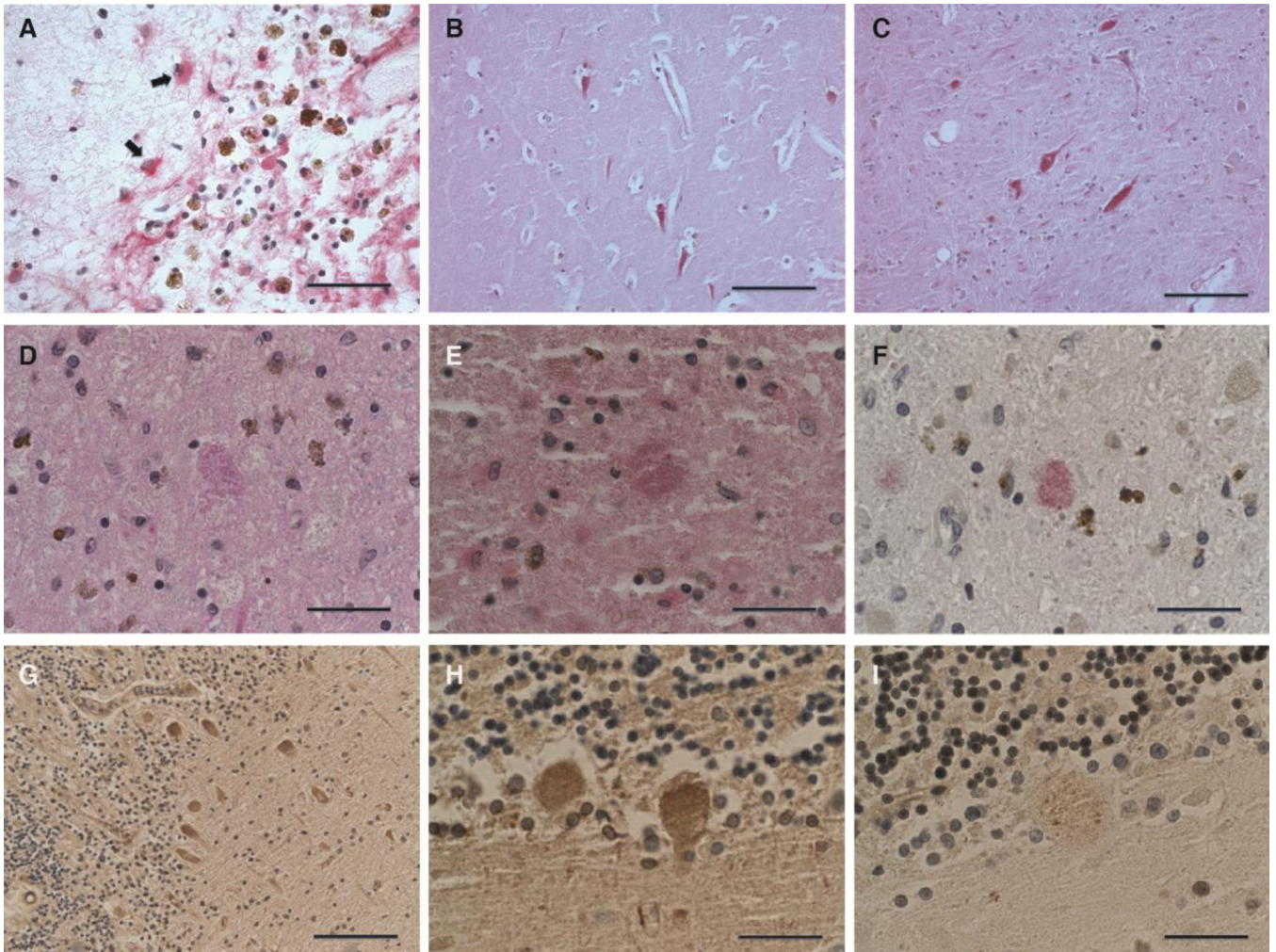


**Figure 5. PKAN-type protein aggregates in other brain regions**

(A) Immunohistochemical staining for apoE demonstrated a high degree of expression in astrocytes (arrows) in reactive conditions, including this cortical infarct, in many regions of the brain; however, neuronal expression was found in limited circumstances in a survey of ischemic lesions (scale: 50  $\mu$ m).

(B) ApoE immunohistochemistry performed on the CA1 sector of the hippocampus of this 47-year-old cognitively intact patient show increased apoE expression in neurons with contracted cytoplasm and loss of nuclear detail, morphologic features of acute terminal ischemia (Vector Red development; scale: 50  $\mu$ m). Additional immunohistochemical staining did not reveal the presence of ubiquitin expression in these neurons (not shown).

(C) ApoE immunohistochemistry performed on condensed ischemic neurons in a section of globus pallidus of a 68-year-old patient with a nearby acute infarct (Vector Red development; scale: 50  $\mu$ m). Acute lesions here also did not demonstrate ubiquitin expression (not shown).

(D–F) A remote infarct involving the pars reticulata of the substantia nigra of an 88-year-old female contains neurons with granular eosinophilic aggregates similar to those of PKAN (D,

H&E/LFB stain), that are shown by tissue immunohistochemistry to contain apoE (E) and ubiquitin (F) (Vector Red development in E and F; scale: 33  $\mu$ m).

(G–I) Immunohistochemical studies of a remote cerebellar infarct in a 76-year-old female showing Purkinje neurons with widespread diffusely increased apoE (G and H) and focal, punctate ubiquitin (I) expression. Immunohistochemical stains were developed with brown chromagen and hematoxylin counterstain (scale: G, 100  $\mu$ m; H and I, 33  $\mu$ m).

Author Manuscript

Author Manuscript

Author Manuscript

Author Manuscript



Clinical and molecular genetic features of PKAN cases used in biochemical and immunohistochemical studies.

**Table. 1**

Case	Sex	Age of onset (y)	Symptoms	Age at death (y)	Mutation	Molecular features
120	Female	1	Dystonia, pigmentary retinopathy	10	c.943_945del(CTT)	In-frame deletion
158	Female	3	Dystonia, parkinsonism	10	c.1231G>A	Missense
23	Male	6	Dystonia, parkinsonism, pigmentary retinopathy	20	1231C>A (hom)	Missense
367	Female	Unknown	Dystonia	8	c.440_441insCT c.943_945del(CTT)	Premature stop codon; In-frame deletion
146	Female	32	Dystonia, parkinsonism	48	c.1231G>A c.370A>G	Premature stop codon; In-frame deletion